

# Exact results for polaron and molecule in one-dimensional spin-1/2 Fermi gas

Runxin Mao(毛润欣),<sup>1</sup> X. W. Guan(管习文),<sup>2,3</sup> and Biao Wu(吴飙)<sup>1,4,5,6,\*</sup>

<sup>1</sup>International Center for Quantum Materials, School of Physics, Peking University, Beijing 100871, China

<sup>2</sup>State Key Laboratory of Magnetic Resonance and Atomic and Molecular Physics, Wuhan Institute of Physics and Mathematics, Chinese Academy of Sciences, Wuhan 430071, China

<sup>3</sup>Department of Theoretical Physics, Research School of Physics and Engineering, Australian National University, Canberra ACT 0200, Australia

<sup>4</sup>Collaborative Innovation Center of Quantum Matter, Beijing 100871, China

<sup>5</sup>Wilczek Quantum Center, College of Science, Zhejiang University of Technology, Hangzhou 310014, China

<sup>6</sup>Synergetic Innovation Center for Quantum Effects and Applications, Hunan Normal University, Changsha 410081, China

Using exact Bethe ansatz (BA) solutions, we show that a spin-down fermion immersed into a fully polarized spin-up Fermi sea with a weak attraction is dressed by the surrounding spin-up fermions to form the one-dimensional analog of a polaron. As the attraction becomes strong, the spin-down fermion binds with one spin-up fermion to form a tightly bound molecule. Throughout the whole interaction regime, a crossover from the polaron to a molecule state is fully demonstrated through exact results of the excitation spectrum, the effective mass, binding energy and kinetic energy. Furthermore, a clear distinction between the polaron and molecule is conceived by the probability distribution, single particle reduced density matrix and density-density correlations, which are calculated directly from the Bethe ansatz wave function. Such a polaron-molecule crossover presents a universal nature of an impurity immersed into a fermionic medium with an attraction in one dimension.

PACS numbers: 03.75.Ss, 03.75.Hh, 02.30.Ik, 05.30.Rt

## I. INTRODUCTION

Advance in trapping and manipulating cold fermionic atoms have provided an experimental realization of various many-body phenomena [1–4]. In particular, the recent observation of Fermi polarons in a three-dimensional (3D) tunable Fermi liquid of ultracold atoms [5–7] provides insightful understanding of quasiparticle physics in many-body systems [8]. The Fermi polaron is a dressed spin-down impurity fermion by the surrounding scattered fermions in a spin-up Fermi sea. With increasing attraction, the single spin-down fermion undergoes a possibly polaron-molecule transition in the fermionic medium in 3D. The study of quasiparticle physics and the dynamics of polarons and molecules in fermionic medium has received much theoretical and experimental attention [5, 6, 9–15]. In this context, all studies concerning the first order nature of the polaron-molecule transition in a 3D fermionic medium [9–11] involve variational ansatz with some approximations that is ultimately not justified in low dimensions [16, 17]. It is therefore highly desirable to have some rigorous results of such quasiparticle physics in different mediums.

For 1D systems, there in general does not exhibit true quasiparticles due to strong collective nature at low temperatures. However, such a collective behavior does not rule out the existence of polarons for very few impurities immersed into the bosonic or fermionic mediums. In

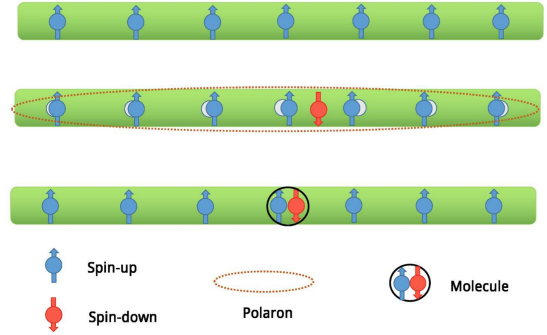


FIG. 1: (color online) Schematic configuration of polaron-molecule crossover of a single attractive impurity in the 1D Fermi gas. In weak attractive limit, the single impurity (red), a spin-down fermion, dressed by the surrounding scattered spin-up fermions (blue) from the medium behaves like a polaron (dashed oval) with an effective mass  $m^* \approx m$ . For strong attraction, it binds with one spin-up fermion from the Fermi sea to a tightly bound molecule (black circle) of two-atom with an effective mass  $m^* \approx 2m$ .

contrast to the Fermi liquid theory for the study of the Fermi polaron in 2D/3D, the exact Bethe ansatz solutions are more capable of capturing microscopic origin of polarons and molecules [18–22, 24, 30]. In this regard, the 1D spin-1/2 delta-function interacting Fermi gas [25, 26] is ideal for the study of quantum impurity problem [4, 18, 19]. The fundamental physics of this model with arbitrary spin population imbalance is determined by a set of transcendental equations which were found by Yang using Bethe ansatz (BA) hypothesis in

\*Electronic address: wubiao@pku.edu.cn

1967 [25]. This model shows many interesting physical properties [4]. Here we show that the exact BA solutions can be used to study the different properties of polarons and molecules in the 1D Fermi gases.

In this paper, using exact Bethe Ansatz (BA) solution, we rigorously study Fermi polaron and molecule states in a 1D fermionic medium. For weak attraction, the single spin-down impurity gets dressed by the surrounding spin-up fermions to form a polaron-like quasiparticle. However, as the attractive interaction grows, the spin-down fermion binds only one spin-up fermion from the medium to gradually form a tightly bound molecule. See a cartoon picture shown in Fig. 1. In comparison with the previous study [19], here we analytically and numerically calculate the polaron energy, the binding energy, the effective mass for this impurity problem. Moreover, we obtain an explicit form of the BA wave function of the single spin-down immersed in the fully-polarized Fermi sea. Using this exact wave function we further calculate the distributions and the correlations of the polaron and molecule which are the major quantities for experimental measurements on these states. Our result provides a microscopic origin of the polarons and molecules resulting in from quantum impurities.

The paper is organized as follows: in Section II, we derive explicit form of the Bethe wave function. In Section III, we analytically and numerically calculate the excitation spectrum with a precise determination of the effective mass and binding energy. In section IV and V we calculate the probability distribution functions and correlation functions. We conclude in Section VI.

## II. MODEL AND BETH WAVE FUNCTION

We study the one dimensional spin-1/2 Fermi gas called Yang-Gaudin model [25, 26], where the fermions interact with each other via the  $\delta$ -function potential. Due to the symmetry of the wave function, the interaction only occurs between two fermions with different spins. The Hamiltonian of the system thus has the following form [25, 26]

$$H = \sum_{\sigma=\downarrow,\uparrow} \int \phi_{\sigma}^{\dagger}(x) \left( -\frac{\hbar^2}{2m} \frac{d^2}{dx^2} \right) \phi_{\sigma}(x) + g_{1D} \int \phi_{\downarrow}^{\dagger}(x) \phi_{\uparrow}^{\dagger}(x) \phi_{\downarrow}(x) \phi_{\uparrow}(x), \quad (1)$$

where  $m$  is the atomic mass,  $g_{1D}$  characterizes the strength of the  $\delta$ -function interaction, and the field operators  $\phi_{\uparrow}$  and  $\phi_{\downarrow}$  describe the fermionic atoms in the states  $|\uparrow\rangle$  and  $|\downarrow\rangle$ , respectively. In this work we focus on the case where a single spin-down fermion resides in the sea of  $N-1$  spin-up fermions.

The system described by the Hamiltonian Eq.(1) is a prototypical integrable model, which has been experimentally realized with ultracold atoms trapped in 1D geometry [27, 28]. In such 1D experiments, the wave guide

atoms are tightly confined in two transverse directions and weakly confined in the axial direction. Consequently, the trapped atoms can be effectively described by the Hamiltonian (1) within the local density approximation [27–29] or by exact strong coupling ansatz wave functions of the trapped gas [30–33]. In these experiments, the coupling constant  $g_{1D}$  can be written as  $g_{1D} = \hbar^2 c/m$  with  $c = -2/a_{1D}$ , where  $a_{1D}$  is the effective 1D scattering length. According to Ref. [34],  $a_{1D}$  is related to the 3D scattering length  $a_{3D}$  as  $a_{1D} = -a_{\uparrow}^2/a_{3D} + Aa_{\uparrow}$ , where  $a_{\uparrow} = \sqrt{\hbar/(m\omega_{\uparrow})}$  is the transverse oscillator length, and  $A \approx 1.0326$  is a constant. For repulsive fermions,  $c > 0$  and for attractive fermions,  $c < 0$ . The Bethe ansatz solutions of the model provide a precise understanding of many-body phenomena and few-body physics, see review [4]. In this paper we focus on the model (1) with attractive interaction and periodic boundary conditions.

The Bethe wave function of the model Eq.(1) is very complicated. With the help of Takahashi's Bethe ansatz wave function [35], we first simplify the Bethe wave function of an energy eigenstate for the case with the  $N$ th fermion being spin-down, i.e.

$$f_{\downarrow N}(x_1, x_2, \dots, x_N) = \sum_{l=1}^N \begin{vmatrix} a_{11} & \dots & a_{1,N-1} \\ \cdot & \cdot & \cdot \\ \cdot & a_{ij} & \cdot \\ \cdot & \cdot & \cdot \\ a_{N-1,1} & \dots & a_{N-1,N-1} \end{vmatrix} e^{ik_l x_N}, \quad (2)$$

where

$$a_{ij} = [k_{l+j} - \lambda + ic' \text{sign}(x_N - x_i)] e^{ik_{l+j} x_i} \quad (3)$$

if  $l + j \leq N$ ; for other cases,

$$a_{ij} = [k_{l+j-n} - \lambda + ic' \text{sign}(x_N - x_i)] e^{ik_{l+j-n} x_i}. \quad (4)$$

The wave function for the four-body case is given explicitly in Appendix A. In the above wave function, we denote  $c' = c/2$ , and  $\lambda$  is the spin rapidity parameter and  $\{k_j\}$  with  $j = 1, 2, \dots, N$  are the quasi-momenta of fermions. They can be determined by the Bethe Ansatz equations [25] (also see below).

The total wave function of our system should be antisymmetric under the permutation of any two fermions. To construct this total wave function, we define

$$f_{\downarrow_j}(x_1, \dots, x_j, \dots, x_N) = -f_{\downarrow N}(x_1, \dots, x_N, \dots, x_j), \quad (5)$$

where the subscript  $\downarrow_j$  means that the  $j$ th fermion is spin-down while the rest of the fermions are spin-up. As a result, the total wave function takes the following form,

$$f_{tot} = \frac{1}{\sqrt{G}} \sum_{j=1}^N f_{\downarrow_j} |\downarrow_j\rangle, \quad (6)$$

and  $G$  is the normalization constant and  $|\downarrow_j\rangle$  denotes a spin state with the  $j$ th spin down and all other spins up.

For solving our problem, we write down the following the BA equations [25]

$$\frac{k_j - \lambda + ic'}{k_j - \lambda - ic'} = \exp(ik_j L), \quad (7)$$

$$\prod_{j=1}^N \frac{k_j - \lambda + ic'}{k_j - \lambda - ic'} = 1. \quad (8)$$

The corresponding eigen-energy is given by

$$E = \sum_{j=1}^N \frac{\hbar^2 k_j^2}{2m}. \quad (9)$$

This problem of  $N - 1$  fermions of the up spin and one fermion of the opposite spin was studied by McGuire in 1965 and 1966 [36, 37], who calculated only the energy shift caused by the extra spin-down fermion. However, the key feature of this impurity problem is the collective behavior of polaron and molecule, which lacks a comprehensive understanding. In the rest of the paper (except Section IV), for convenience and without loss of generality, we consider only the cases where  $N$  is even.

### III. POLARON AND MOLECULE

When a single attractive impurity is immersed in the fully-polarized Fermi sea, an intuitive picture immediately arises as illustrated schematically in Fig. 1. The single impurity will be addressed by a cloud of fermions due to attraction. When the impurity moves, it will drag these fermions along. Effectively, it can be regarded as a new particle with a different mass moving freely. This is the well known polaron. When the attraction becomes very strong, the impurity can pair with one fermion to form a molecule. This nature is reflected by Haldane generalized exclusion statistics [38–42], i.e. the statistical interaction and dynamical interaction are transmutable in 1D. For a weak attraction, we see that the quasimomentum of a spin-down fermion essentially depends on that of all spin-up fermions. This gives a statistical nature of polaron, namely mutual statistics [39, 43]. Whereas for a strong attraction, the spin-down fermion tightly bounds with a spin-up fermion from the fully-polarized Fermi sea. In this circumstance, the statistics of the bond pair reveals a non-mutual statistics.

To rigorously establish such a transition, we examine the energy shift caused by the impurity and see how it changes with the interaction strength. When there is no interaction, the single spin-down fermion can share a momentum with a spin-up fermion. This implies mathematically that there exists a pair of  $k$ 's, say,  $k_{N-1}$  and  $k_N$ , such that  $k_{N-1} = k_N = p$ . When the attractive interaction between spin-up fermion and spin-down fermion is turned on, these two momenta can become a pair of complex conjugates,  $k_{N-1, N} = p \pm i\beta$ , indicating the formation of a polaron or molecule.

#### A. Weak coupling

We first consider the weak coupling limit,  $L|c| \ll 1$ . In this limit, it is straightforward to find that  $p \approx \lambda$  and  $\beta \approx \sqrt{|c|/L}$ . With these two facts [19], we can readily obtain from Eq.(7) and Eq.(8)

$$p \approx \frac{2n_p \pi}{L} - \frac{1}{2} \sum_{j=1}^{N-2} \frac{|c|}{2(n_p - n_j)\pi} \quad (10)$$

$$k_j \approx \frac{2n_j \pi}{L} - \frac{|c|}{2(n_j - n_p)\pi}, \quad (j = 1, \dots, N-2) \quad (11)$$

where  $n_j$ 's and  $n_p$  are integers and  $n_j \neq n_p$ . According to the Fermi statistics, for the lowest energy state, we have  $n_j = \pm 1, \pm 2, \dots, (N-2)/2$  (for details see Appendix B). From the above equations, we can calculate the energy of the system with a single spin-down fermion

$$\begin{aligned} E &= \frac{\hbar^2}{2m} \left( -2\beta^2 + 2p^2 + \sum_{j=1}^{N-2} k_j^2 \right) \\ &\approx -\frac{\hbar^2}{2m} \frac{2(N-1)|c|}{L} + \frac{\hbar^2 q^2}{2m} + E_0, \end{aligned} \quad (12)$$

where  $q = 2n_p \pi / L$  and  $E_0$  is the ground state energy of the system when there is no interaction, that is,  $c = 0$ . For  $n_p = 0$ , we recover the ground state energy of the gas with  $N - 1$  spin-up fermions and one spin-down fermion given by McGuire [36, 37].

The energy expression (12) naturally gives the dispersion of a polaron-like quasiparticle moving slowly in the fully polarized Fermi sea. It provides a rich insight into such collective nature of polaron: 1) the first term is the mean binding energy, showing that the spin-down fermion experiences a mean field attraction from the fully polarized Fermi sea; 2) the second term is the kinetic energy of a single classical particle with momentum  $\hbar q$  and mass  $m$ . When  $c = 0$ , this is just the kinetic energy for the newly added spin-down fermion. When  $c \neq 0$  but small, this kinetic energy does not change its form even though the spin-down fermion is interacting with spin-up fermions and has lost its individual character. In this regard, one can view the spin-down fermion addressed by the surround spin-up fermions as a polaron. In one dimension, such a polaronic behaviour is a typical elementary excitation with infinite lifetime due to the reshuffle of the eigenstates in excitations. When  $c$  becomes bigger, the effective mass of the polaron will be different from the bare mass  $m$  (the leading order contribution is proportional to  $c^2$ ), but overall picture remains the same: a Fermi sea, a binding energy  $E_b = -\frac{\hbar^2}{2m} \frac{2(N-1)|c|}{L}$ , and a classical particle with an effective mass  $m^*$ .

The above results are valid up to the first order of  $cL$ . The results to the second order of  $cL$  can be found in the Appendix B. There is a correction to the binding energy. However, it is very hard to calculate the effective mass of the polaron for the order over the first order of  $cL$ .

### B. Strong coupling

We now consider the strong coupling limit,  $|c|L \gg 1$ . Using  $(|c|L)^{-1}$  as the perturbation parameter [19], we find  $p$  and the  $N - 2$  real momenta

$$p \approx \frac{n_p \pi}{L} - \sum_{j=1}^{N-2} \frac{2n_j \pi}{|c|L} + \frac{2(N-2)n_p \pi}{|c|L} \quad (13)$$

$$k_j \approx \frac{n_j \pi}{L} + \frac{4n_j \pi - 4n_p \pi}{|c|L} \quad (14)$$

with  $n_j = \pm 1, \pm 3, \dots, \pm (N - 3)$  and  $n_p$  is an arbitrary integer. In addition, we find  $\beta \approx |c|/2$ . Therefore, the total energy is

$$\begin{aligned} E &= \frac{\hbar^2}{2m} \left( -2\beta^2 + 2p^2 + \sum_{j=1}^{N-2} k_j^2 \right) \\ &= -\frac{\hbar^2}{2m} \left[ \frac{c^2}{2} + \left(1 + \frac{8}{|c|}\right) \frac{(2N-1)(N-2)\pi^2}{L^2} \right] \\ &\quad + \left[ \frac{1}{2} + \frac{2(N-2)}{|c|} \right] \frac{\hbar^2 q^2}{2m} + \left(1 + \frac{8}{|c|}\right) E_0. \end{aligned} \quad (15)$$

Similar to the case of weak coupling, this energy has three terms: the binding energy, the kinetic energy, and the Fermi sea energy. However, all of them are different, and even the Fermi sea energy is slightly modified by the strong interaction. In particular, the kinetic energy can be regarded as a quasi-particle with effective mass

$$m^* \approx 2m \left( 1 - \frac{4(N-2)}{L|c|} \right), \quad (16)$$

which is almost twice the bare mass  $m$ . After a subtraction of the ground state energy and chemical potential within Eq. (15), we obtain the binding energy of the molecule state

$$E_b = \frac{\hbar^2}{2m} \left\{ -\frac{c^2}{2} + \frac{8\pi^2}{3|\gamma|} \right\}, \quad (17)$$

where  $\gamma = c/n$  is a dimensionless interaction strength

### C. General case

The above two limiting cases show that the total energy of the system can be divided into three parts,

$$E = E_0 + E_b + \frac{\hbar^2 q^2}{2m^*}. \quad (18)$$

$E_0$  is the Fermi sea energy, the ground state energy of  $N$  free fermions;  $E_b$  is the binding energy; the last term is the kinetic energy of the quasi-particle, i.e. dispersion of a polaron. In the weak coupling limit, the binding energy is

$$E_b \approx -\frac{\hbar^2}{2m} \frac{2|c|}{L} (N-1) = 2\gamma \frac{\hbar^2 n^2}{2m}, \quad (19)$$

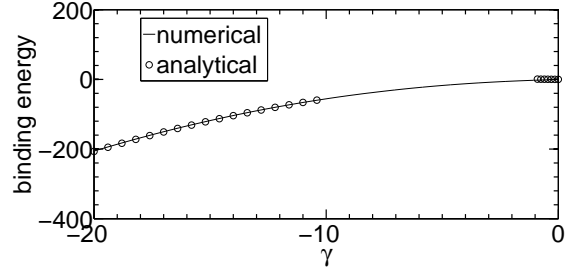


FIG. 2: Binding energy  $E_b$ . The solid line is the numerical result and the circles stand the result from the analytical expression (17) and (19) for strong and weak attractions, respectively. The unit of energy is  $\frac{\hbar^2 n^2}{2m}$  and  $\gamma$  is the dimensionless interaction strength.  $N = 10$ ,  $L = 1$ .

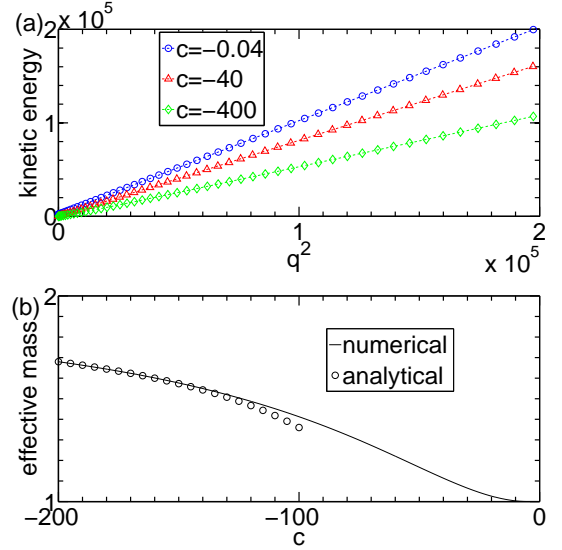


FIG. 3: (color online) (a) The kinetic energy as a function of the square of the momentum  $q$  for different values of interaction strength. The unit of energy is  $\hbar^2/(2mL^2)$  and the unit of  $q^2$  is  $L^{-2}$ . (b) Effective mass  $m^*/m$  as a function of interaction strength  $c$ . The line is the numerical result and the circles denote the analytical result obtained from (16) for strong coupling regime. For weak coupling regime, the leading order contribution to the effective mass is identified as an order of  $c^2$ . The mass ratio  $m^*/m$  has no unit and the unit of  $c$  is  $L^{-1}$ . Here  $N = 10$  and  $L = 1$ .

where  $n = N/L$  is the density of particle. In the strong coupling limit, the binding energy is given by (17).

A crossover from a polaron to the molecule is seen for an intermediate interaction strength, i.e. the total energy of this system can be divided into three parts as indicated in (18). However, in general, the BA equations in Eq.(7,8) can not be solved analytically. We have to resort to numerical method. To compute the binding energy  $E_b$ , we compute the ground state of the system and then subtract out  $E_0$ . The numerical results with  $N = 10$ ,  $L = 1$  are shown in Fig. 2. We observe that our numerical results agree well with analytical expressions

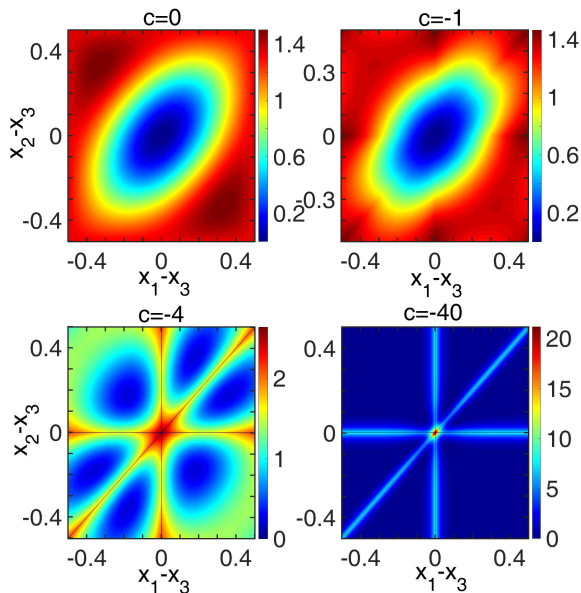


FIG. 4: (color online) Probability distribution of the ground state in the case of three fermions for  $c = 0, -1, -4, -40$ . When  $c = 0$ , the ground state corresponds to  $\{k_1, k_2, k_3\} = \{0, 0, 2\pi/L\}$ . Here the distribution unit is  $L^{-3}$ .

(17) and (19) in the weak and strong coupling limits.

For the kinetic energy, we compute the system energy for a given momentum  $q$  and then subtract out  $E_0$  and  $E_b$ . The results are plotted in Fig. 3 (a), where the kinetic energy is seen to grow as a power of  $q^2$ . By extracting the slope, we can compute the effective mass  $m^*$ , which is shown in Fig. 3 (b). In the weak coupling limit, we indeed see that  $m^*$  approaches to the bare mass  $m$ . In the strong coupling limit, the numerical result of  $m^*$  agrees well with our analytical result (16), i.e.  $m^* \approx 2m(1 - \frac{4}{|\gamma|})$ . These results fully confirm the polaron behavior in the problem of such a spin-down fermion immersed into a fully-polarized Fermi sea in 1D.

#### IV. PROBABILITY DISTRIBUTION FUNCTION OF THREE FERMIONS

It is interesting to see how these polarons or molecules look like from weak to strong interactions. For this purpose, we need to plot the wave function in the real space. Due to the reason that the visual dimensions are restricted to up to three dimension, therefore we can at most plot the wave function of three fermions. To further simplify the situation, we plot the probability distribution for fixing one of the fermions at  $x_3 = L/2$ . From Eq.(6), we have the distribution function

$$\begin{aligned} \rho(x_1, x_2) &= |f_{tot}(x_1, x_2, L/2)|^2 \\ &= \frac{1}{G} \left\{ |f_{\downarrow_1}(x_1, x_2, L/2)|^2 + |f_{\downarrow_2}(x_1, x_2, L/2)|^2 \right. \\ &\quad \left. + |f_{\downarrow_3}(x_1, x_2, L/2)|^2 \right\}. \end{aligned} \quad (20)$$

Here  $G$  is the normalization factor.

We focus on the ground state. In the case of  $c = 0$ , this means that we have  $\{k_1, k_2, k_3\} = \{0, 0, 2\pi/L\}$  and

$$\begin{aligned} \rho(x_1, x_2) &= \frac{1}{L^3} \left\{ 1 + \frac{1}{3} \cos\left(\frac{2\pi}{L}x_1\right) + \frac{1}{3} \cos\left(\frac{2\pi}{L}x_2\right) \right. \\ &\quad \left. - \frac{1}{3} \cos\left[\frac{2\pi}{L}(x_1 - x_2)\right] \right\}. \end{aligned} \quad (21)$$

The probability distributions are plotted for four different values of  $c$  in Fig. 4. When  $c = 0$ , the probability is the smallest one in the vicinity of  $x_1 = x_2 = x_3$  since the three fermions do not like to cluster together. For the weak attraction,  $c = -1$ , the probability distribution looks very similar to the case  $c = 0$ . However, as the attraction gets stronger, the distribution changes dramatically. As shown in Fig. 4, for  $c = -4$ , there is a concentrated red area around the point  $x_1 = x_2 = x_3$ , implying that the two fermions form a bound pair which tends to stay with the excess fermion under a strong attraction. This is a clear indication of the crossover region from a polaron to a molecule. When the attraction is very strong, e.g.,  $c = -400$ , the probability is significantly different from zero only in a small area around  $x_1 = x_2 = x_3$  and around the three lines,  $x_1 = x_3, x_2 = x_3, x_1 = x_2$ . This signals the formation of a molecule. Note that the probability is exactly zero at  $x_1 = x_2 = x_3$  due to the Fermi statistics.

## V. CORRELATIONS

With the wave function in Eq.(6), we can compute various correlation functions, from which we can gain more insights into the properties of polarons and molecules. We focus on the one-body correlation function [44, 45] and the density-density correlation function [46, 48].

### A. One-body correlation function

The one-body correlation function is in fact the reduced one-body density matrix. It can be regarded as the probability of creating a particle at the position  $x$  while annihilating a particle at the position  $x'$  at the same time. For our system, there are two types of such a correlation function,  $\langle a_{\uparrow}^+(x)a_{\downarrow}(x') \rangle$  and  $\langle a_{\uparrow}^+(x)a_{\uparrow}(x') \rangle$ . The former is clearly zero since we cannot annihilate one spin-down fermion at  $x'$  and create one spin-up fermion at  $x$ . For the latter, without loss of generality, we set  $x' = L/2$  and have

$$\begin{aligned} \langle a_{\uparrow}^+(x)a_{\uparrow}(L/2) \rangle &= \frac{1}{G} \int \cdots \int dx_2 \cdots dx_N \left\{ \right. \\ &\quad \left. \sum_{j=2}^N f_{\downarrow_j}^*(x, x_2, \cdots, x_N) f_{\downarrow_j}(L/2, x_2, \cdots, x_N) \right\}. \end{aligned} \quad (22)$$

Here the wave function was normalized.

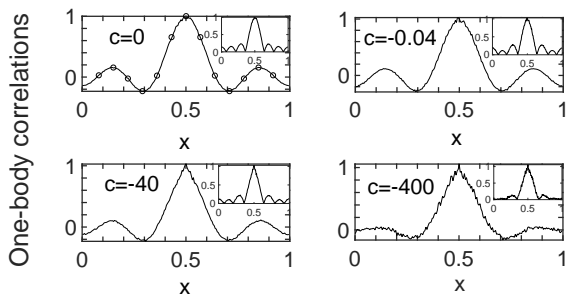


FIG. 5: One-body correlations of the ground state at  $c = 0, -0.04, -40, -400$ . When  $c = 0$ , the momenta are  $\{0, 0, \pm 2\pi, \pm 4\pi, \pm 6\pi\}$ . The black lines are the numerical results of the real part of the correlation function; the hollow circles denote the analytical results of  $c = 0$ . The insets show the absolute values of the one-body correlations for  $N = 8$ . Here the unit of correlations is  $L^{-1}$ .

When  $c = 0$ , we can easily calculate the correlation function

$$\begin{aligned} \langle a_{\uparrow}^{\dagger}(x)a_{\uparrow}(\frac{L}{2}) \rangle &= \frac{1}{L} \left\{ \frac{(-1)^{\frac{N-2}{2}} \cos[\frac{(N-1)\pi x}{L}]}{N-1} \right\} \\ &\approx \frac{1}{L} \left\{ \frac{(-1)^{\frac{N}{2}} \cos(k_F x)}{N} \right\}, \end{aligned} \quad (23)$$

where  $k_F = N\pi/L$  is the Fermi wave-vector of the system. When  $c \neq 0$ , we have to rely on the numerical method, except the limit cases [47]. The multi-dimensional integration in Eq.(22) is done with the Monte Carlo (MC) method and the results for  $N = 8$  are shown Fig. 5. In general, the one-body correlation function is complex. For the cases studied here, the imaginary parts of the correlation functions are small. Therefore, shown in Fig. 5 are the real parts of the one-body correlation functions; the absolute values are shown in the insets.

The correlation functions for different values of interaction strength in Fig. 5 show peaks around  $x = L/2$  and then decay off over large distance, a common feature of all correlation functions. Their decay tails are oscillatory. The oscillation period is  $2\pi/k_F$ , as indicated in Eq.(23), and it changes little as the attractive interaction gets stronger. The absolute values of the correlation function show in the insets, where the oscillation period is  $\pi/k_F$ , which is the same as the Friedel oscillations[49]. This is expected as the cause of the oscillations in Fig. 5 and also as the cause of the Friedel oscillations.

Another interesting feature in Fig. 5 is that the correlation decays faster when the attractive interaction gets stronger.

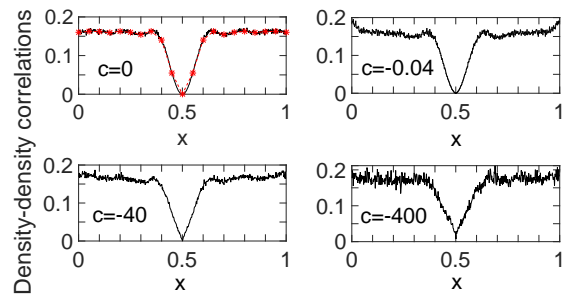


FIG. 6: (color online) Density-density correlations between up spins in the ground state for  $c = 0, -0.04, -40, -400$ . When  $c = 0$ , the momenta are  $\{0, 0, \pm 2\pi, \pm 4\pi, \pm 6\pi\}$ . The black lines are the numerical results; the red line is the analytical result of  $c = 0$ .  $N = 8$ . The unit of length is  $L$  and the unit of correlations is  $L^{-2}$ .

## B. Density-density correlation functions

There are two types of density-density correlations, one between up spins and the other between up and down spins. The density-density correlation between up spins is

$$\begin{aligned} \langle a_{\uparrow}^{\dagger}(x)a_{\uparrow}(x)a_{\uparrow}^{\dagger}(\frac{L}{2})a_{\uparrow}(\frac{L}{2}) \rangle &= \int \cdots \int dx_3 \cdots dx_N \\ &\frac{1}{G} \left\{ \sum_{j=3}^N f_{\downarrow j}^*(x, \frac{L}{2}, x_3, \cdots, x_N) f_{\downarrow j}(x, \frac{L}{2}, x_3, \cdots, x_N) \right\}. \end{aligned} \quad (24)$$

This correlation function indicates a probability to find a spin-up fermion at  $x$  when there is a spin-up fermion at  $L/2$ . When  $c = 0$ , this correlation function is calculated in a straight forward way

$$\begin{aligned} &\langle a_{\uparrow}^{\dagger}(x)a_{\uparrow}(x)a_{\uparrow}^{\dagger}(\frac{L}{2})a_{\uparrow}(\frac{L}{2}) \rangle \\ &= \frac{1}{L^2} \left\{ \frac{N-1}{N-2} - \frac{\cos[\frac{(2N-3)\pi x}{L}]}{2(N-1)(N-2) \cos(\frac{\pi x}{L})} \right. \\ &\quad \left. + \frac{\sin(\frac{\pi x}{L}) \sin[\frac{(2N-3)\pi x}{L}] - 1}{2(N-1)(N-2) \cos^2(\frac{\pi x}{L})} \right\} \\ &\approx \frac{1}{L^2} \left\{ 1 + \frac{\cos(2k_F x + \frac{\pi x}{L})}{2N^2 \cos(\frac{\pi x}{L})} \right. \\ &\quad \left. + \frac{\sin(\frac{\pi x}{L}) \sin(2k_F x + \frac{\pi x}{L}) - 1}{2N^2 \cos^2(\frac{\pi x}{L})} \right\}. \end{aligned} \quad (25)$$

As shown in Fig.6, this function is zero at  $x = L/2$  and approaches a constant when  $x$  is far away from  $L/2$ . The zero value of the density-density correlation at  $x = L/2$  is due to the Pauli exclusion principle: there can only be one fermion with up spin at  $x = L/2$ . When  $x$  is far away from  $L/2$ , the effect of the exclusion principle becomes weak and the probability to find another up-spin fermion becomes a constant as the system is in uniform.

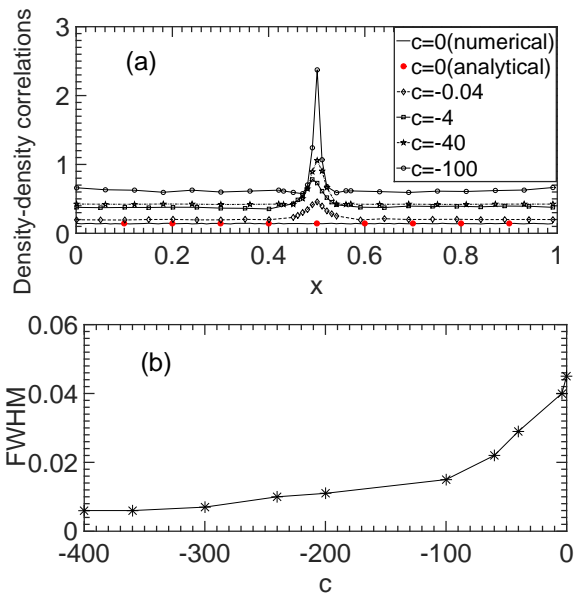


FIG. 7: (color online) (a) Density-density correlations between up spin and down spin in the ground state for  $c = 0, -0.04, -4, -40, -100$ . For clarity, the curves for  $c \neq 0$  have shifted upwards by 0.1, 0.2, 0.3, 0.4, respectively. When  $c = 0$ , the momenta are  $\{0, 0, \pm 2\pi, \pm 4\pi, \pm 6\pi\}$ . The different symbol lines are the numerical results for different interaction; the red circles are the analytical result for  $c = 0$ . (b) The full width at half maximum (FWHM) as a function of the interaction strength  $c$ .  $N = 8$ . The unit of length is  $L$ , the unit of correlations is  $L^{-2}$  and the unit of  $c$  is  $L^{-1}$ .

When  $c \neq 0$ , the density-density correlations are computed numerically and the results are plotted in Fig.6 for  $N = 8$ . We observe in this figure that the interaction does not change the overall feature of the correlation function. It appears that the amplitude of the oscillatory tail is suppressed by the strong interaction. However, due to the limitation of the accuracy of the numerical results, it is hard to quantify this suppression.

The density-density correlations between up spin and down spin is

$$\begin{aligned}
 & \langle a_{\uparrow}^+(x)a_{\uparrow}(x)a_{\downarrow}^+(\frac{L}{2})a_{\downarrow}(\frac{L}{2}) \rangle \\
 &= \frac{1}{G} \sum_{j=2}^{N-1} \int \cdots \int dx_2 \cdots dx_{j-1} dx_{j+1} \cdots dx_N \\
 & \left\{ f_{\downarrow N}^*(x, x_2, \cdots, x_{j-1}, \frac{L}{2}, x_{j+1}, \cdots, x_N) \times \right. \\
 & \left. f_{\downarrow N}(x, x_2, \cdots, x_{j-1}, \frac{L}{2}, x_{j+1}, \cdots, x_N) \right\}, \tag{26}
 \end{aligned}$$

which gives us the probability to find a spin-up fermion at  $x$  when there is a spin-down fermion at  $\frac{L}{2}$ . When  $c = 0$ , this density-density correlations is a constant and equal to  $1/[(N-1)L^2]$ . This reflects the fact that when there is no interaction the presence of a down-spin fermion does

not affect the density of up-spin fermions. When  $c \neq 0$ , the correlation functions are computed numerically and the results are shown in Fig.7 (a) for  $N = 8$ . From the figure, we see that a peak immediately emerges when the attractive interaction is turned on. This is resulted from the formation of polaron. As the interaction gets stronger and stronger, the peak becomes narrower and narrower. This signature indicates a crossover from the polaron-like behaviour to the tightly bound molecule. Furthermore, the full widths at half maximum (FWHM) as a function of interaction strength is plotted in Fig.7 (b).

The density-density correlation function characterizes the interference of two particles. The measurement of many-body correlations was carried out for bosons via a single atom detector, where the many-body Wick's theorem provides a significant theoretical input [52]. It is highly desirable to adapt this experimental technique to measure many-body correlations for interacting fermions. On the other hand, in the cold atoms experiments, one can overlap a TOF image with its copy that is shifted by  $x$ . Integrating over the overlapped region, then one may measure the density-density correlation of  $x$ . In fact, in current experiments with ultracold atoms, the ratio frequency spectroscopy of the ultracold atoms is often used to demonstrate the quasiparticle behaviour of the impurity problems [5-7, 53, 54]. The shifts and widths of the spectra are conveniently used to read off the average binding energy and lifetime of polaron. To this end, the spectral function  $A(k, \omega)$ , which gives the probability to find the state with a frequency  $\omega$  and momentum  $\hbar k$ , is a central importance in the problems of this kind. Once we turn on the interaction, the spectral function  $A(k, \omega)$  thus contains Lorentzian peaks. However, the spectral function is related to the single-particle Green's function (retarded Green's function), i.e.,  $A(k, \omega) = \frac{-1}{\pi} \text{Im} G_{\text{ret}}(k, \omega)$ , is cumbersome for computing in general. We will consider this study elsewhere.

## VI. CONCLUSION

We have studied the formation of polaron and molecule when one spin-down fermion is placed in a sea of free up-spin fermions. It shows that as the attractive interaction between up-spin and down-spin fermions increases, the spin-down fermions is dressed up by the surrounding ones from the Fermi sea to form a polaron. Whereas, for an strong attraction the single spin-down fermion tightly bounds one spin-up fermion to form a molecule. We have obtained analytically the effective masses, binding energies and kinetic energies of the polaron and molecule. We have also numerically calculated these key properties for a whole interacting regime. The numerical results confirm the novel nature of the crossover from polaron to molecule in the 1D impurity problem. For the further study of this problem, we have numerically calculated the probability distribution function and the one-body and density-density correlation functions from which the na-

ture of the polaron and molecule in 1D is demonstrated. Our results provide a precise understanding of such typical collective many-body phenomenon caused by quantum impurity. Our method can be directly apply to the impurity problems in different mediums with integrability.

### Acknowledgments

We acknowledge helpful discussion with Yuzhu Jiang. This work is supported by the NBRP of China

(2013CB921903,2012CB921300) and the NSF of China (11274024,11334001,11429402,11374331,11534014).

- 
- [1] M. Lewenstein, A. Sanpera, V. Ahufinger, B. Damski, A. Sen, and U. Sem, *Adv. Phys.* **56**, 243 (2007).
- [2] S. Giorgini, L. P. Pitaevskii, and S. Stringari, *Rev. Mod. Phys.* **80**, 1215 (2008).
- [3] M. A. Cazalilla, R. Citro, T. Giamarchi, E. Orignac, and M. Rigol, *Rev. Mod. Phys.* **83**, 1405 (2011).
- [4] X.-W. Guan, M. T. Batchelor, and C.-H. Lee, *Rev. Mod. Phys.* **85**, 1633 (2013).
- [5] A. Schirotzek, C.-H. Wu, A. Sommer, and M. W. Zwierlein, *Phys. Rev. Lett.* **102**, 230402 (2009).
- [6] N. Navon, S. Nascimbène, F. Chevy, and C. Salomon, *Science* **328**, 729 (2010).
- [7] C. Kohstall, M. Zaccanti, M. Jag, A. Trenkwalder, P. Massignan, G. M. Bruun, F. Schreck, and R. Grimm, *Nature* **485**, 615 (2012).
- [8] P. Massignan, M. Zaccanti, and G. M. Bruun, *Rep. Prog. Phys.* **77**, 034401 (2014).
- [9] S. Nascimbène, N. Navon, K. J. Jiang, L. Tarruell, M. Teichmann, J. McKeever, F. Chevy, and C. Salomon, *Phys. Rev. Lett.* **103**, 170402 (2009).
- [10] R. Combescot and S. Giraud, *Phys. Rev. Lett.* **101**, 050404 (2008).
- [11] G. M. Bruun and P. Massignan, *Phys. Rev. Lett.* **105**, 020403 (2010).
- [12] C. J. M. Mathy, M. M. Parish, and D. A. Huse, *Phys. Rev. Lett.* **106**, 166404 (2011).
- [13] J. Levinsen, P. Massignan, F. Chevy, and C. Lobo, *Phys. Rev. Lett.* **109**, 075302 (2012).
- [14] W. Yi and X. Cui, *Phys. Rev. A* **92**, 013620 (2015).
- [15] R. Schmidt, H. R. Sadeghpour, and E. Demler, *Phys. Rev. Lett.* **116**, 105302 (2016).
- [16] M. M. Parish, *Phys. Rev. A* **83**, 051603(R) (2011).
- [17] S. Giraud and R. Combescot, *Phys. Rev. A* **79**, 043615 (2009).
- [18] J. B. McGuire, *J. Math. Phys.* **6**, 432 (1965); *J. Math. Phys.* **7**, 123 (1966).
- [19] X.-W. Guan, *Frontier of Physics*, **7**, 8 (2012).
- [20] G. E. Astrakharchik and I. Brouzos, *Phys. Rev. A* **88**, 021602 (2013).
- [21] A. S. Dehkharghani, A. G. Volosniev, and N. T. Zinner, *Phys. Rev. A* **92**, 031601(R) (2015).
- [22] S. E. Gharashi, X. Y. Yin, Y. Yan, and D. Blume, *Phys. Rev. A* **91**, 013620 (2015).
- [23] N. J. S. Loft, L. B. Kristensen, A. E. Thomsen, and N. T. Zinner, *J. Phys. B: At. Mol. Opt. Phys.* **49**, 125305 (2016).
- [24] E. V. H. Doggen, A. Korolyuk, P. Törmä, and J. J. Kinnunen, *Phys. Rev. A* **89**, 053621 (2014).
- [25] C. N. Yang, *Phys. Rev. A* **19**, 1312 (1967).
- [26] M. Gaudin, *Phys. Lett. A* **24**, 55 (1967).
- [27] Y.-A. Liao, A. S. C. Rittner, T. Paprotta, W. Li, G. B. Partridge, R. G. Hulet, S. K. Baur, and E. J. Mueller, *Nature (London)* **467**, 567 (2010).
- [28] A. N. Wenz, G. Zürn, S. Murmann, I. Brouzos, T. Lompe, and S. Jochim, *Science* **342**, 457 (2013).
- [29] G. Pagano, M. Mancini, G. Cappellini, P. Lombardi, F. Schäfer, H. Hu, X.-J. Liu, J. Catani, C. Sias, M. Inguscio, and L. Fallan, *Nat. Phys.* **10**, 198 (2014).
- [30] N. J. S. Loft, L. B. Kristensen, A. E. Thomsen, and N. T. Zinner, *J. Phys. B: At. Mol. Opt. Phys.* **49**, 125305 (2016).
- [31] Seyed Ebrahim Gharashi and D. Blume, *Phys. Rev. Lett.* **111**, 045302 (2013).
- [32] F. Deuretzbacher, D. Becker, J. Bjerlin, S. M. Reimann, and L. Santos, *Phys. Rev. A* **90**, 013611 (2014).
- [33] A. G. Volosniev, D. Petrosyan, M. Valiente, D. V. Fedorov, A. S. Jensen, and N. T. Zinner, *Phys. Rev. A* **91**, 023620 (2015).
- [34] M. Olshanii, *Phys. Rev. Lett.* **81**, 938 (1998).
- [35] M. Takahashi, *Thermodynamics of one dimensional solvable models*, Cambridge University Press, Cambridge, (1999).
- [36] J. B. McGuire, *J. Math. Phys.* **6**, 432 (1965).
- [37] J. B. McGuire, *J. Math. Phys.* **7**, 123 (1966).
- [38] F. D. M. Haldane, *Phys. Rev. Lett.* **67**, 937 (1991).
- [39] Y.-S. Wu, *Phys. Rev. Lett.* **73**, 922 (1994); D. Bernard and Y.-S. Wu, *cond-mat/9404025*.
- [40] Z. N. C. Ha, *Phys. Rev. Lett.* **73**, 1574 (1994).
- [41] M. V. N. Murthy and R. Shankar, *Phys. Rev. Lett.* **73**, 3331 (1994).
- [42] C. Nayak and F. Wilczek, *Phys. Rev. Lett.* **73**, 2740 (1994).
- [43] M. T. Batchelor, X.-W. Guan, and N. Oelkers, *Phys. Rev. Lett.* **96**, 210402 (2006).
- [44] C.-M. Chang, W.-C. Shen, C.-Y. Lai, P. Chen, and D.-W. Wang, *Phys. Rev. A* **79**, 053630 (2009).
- [45] A.-W. de Leeuw, H. T. C. Stoof, and R. A. Duine, *Phys. Rev. A* **89**, 053627 (2014).
- [46] J.-S. Caux and P. Calabrese, *Phys. Rev. A* **74**, 031605 (2006).
- [47] EJKP Nandani, R. A. Römer, S. Tan, and X.-W. Guan, *New J. Phys.* **18**, 055014 (2016).

- [48] A. Y. Cherny and J. Brand, Phys. Rev. A **79**, 043607 (2009).
- [49] L. Mao and B. Wu, Surface Science **605**, 1230 (2011).
- [50] X.-W. Guan, M. T. Bathelor, C. Lee, and M. Bortz, Phys. Rev. B **76**, 085120 (2007).
- [51] A. Guidini, G. Bertaina, D. E. Galli, and P. Pieri, Phys. Rev. A **91**, 023603 (2015).
- [52] R.G. Dall, A.G. Manning, S.S. Hodgman, Wu RuGway, K.V. Kheruntsyan, and A.G. Truscott, Nat. Phys. **9**, 341 (2013).
- [53] N. B. Jørgensen, Lars Wacker, Kristoffer T. Skalmstang, Meera M. Parish, Jesper Levinsen, Rasmus S. Christensen, Georg M. Bruun, and Jan J. Arlt, Phys. Rev. Lett. **117**, 055302 (2016).
- [54] M.-G. Hu, M. J. Van de Graaff, D. Kedar, J. P. Corson, E. A. Cornell, and D. S. Jin, Phys. Rev. Lett. **117**, 055301 (2016).

## Appendix A: The four-body wave function

The wave function for the four-fermion case is

$$\begin{aligned}
& f_{\downarrow 4}(x_1, x_2, x_3, x_4) \\
= & \begin{vmatrix} (k_2 - \tilde{\lambda})e^{ik_2x_1} & (k_3 - \tilde{\lambda})e^{ik_3x_1} & (k_4 - \tilde{\lambda})e^{ik_4x_1} \\ (k_2 - \tilde{\lambda})e^{ik_2x_2} & (k_3 - \tilde{\lambda})e^{ik_3x_2} & (k_4 - \tilde{\lambda})e^{ik_4x_2} \\ (k_2 - \tilde{\lambda})e^{ik_2x_3} & (k_3 - \tilde{\lambda})e^{ik_3x_3} & (k_4 - \tilde{\lambda})e^{ik_4x_3} \end{vmatrix} e^{ik_1x_4} \\
+ & \begin{vmatrix} (k_3 - \tilde{\lambda})e^{ik_3x_1} & (k_4 - \tilde{\lambda})e^{ik_4x_1} & (k_1 - \tilde{\lambda})e^{ik_1x_1} \\ (k_3 - \tilde{\lambda})e^{ik_3x_2} & (k_4 - \tilde{\lambda})e^{ik_4x_2} & (k_1 - \tilde{\lambda})e^{ik_1x_2} \\ (k_3 - \tilde{\lambda})e^{ik_3x_3} & (k_4 - \tilde{\lambda})e^{ik_4x_3} & (k_1 - \tilde{\lambda})e^{ik_1x_3} \end{vmatrix} e^{ik_2x_4} \\
+ & \begin{vmatrix} (k_4 - \tilde{\lambda})e^{ik_4x_1} & (k_1 - \tilde{\lambda})e^{ik_1x_1} & (k_2 - \tilde{\lambda})e^{ik_2x_1} \\ (k_4 - \tilde{\lambda})e^{ik_4x_2} & (k_1 - \tilde{\lambda})e^{ik_1x_2} & (k_2 - \tilde{\lambda})e^{ik_2x_2} \\ (k_4 - \tilde{\lambda})e^{ik_4x_3} & (k_1 - \tilde{\lambda})e^{ik_1x_3} & (k_2 - \tilde{\lambda})e^{ik_2x_3} \end{vmatrix} e^{ik_3x_4} \\
+ & \begin{vmatrix} (k_1 - \tilde{\lambda})e^{ik_1x_1} & (k_2 - \tilde{\lambda})e^{ik_2x_1} & (k_3 - \tilde{\lambda})e^{ik_3x_1} \\ (k_1 - \tilde{\lambda})e^{ik_1x_2} & (k_2 - \tilde{\lambda})e^{ik_2x_2} & (k_3 - \tilde{\lambda})e^{ik_3x_2} \\ (k_1 - \tilde{\lambda})e^{ik_1x_3} & (k_2 - \tilde{\lambda})e^{ik_2x_3} & (k_3 - \tilde{\lambda})e^{ik_3x_3} \end{vmatrix} e^{ik_4x_4}
\end{aligned} \tag{A1}$$

where  $\tilde{\lambda} = \lambda - ic' \text{sign}(x_4 - x_i)$ , ( $i$  is the indice of  $k$  in one term).

## Appendix B: Analytical solutions of the Bethe ansatz equations

In this Appendix, we offer detailed derivation for the solutions of the Bethe ansatz (BA) equations Eqs.(7,8) up to the second order in both the weak and strong interaction limits. To simplify the notations, we make the following change of variables:

$$\tilde{k}_j = k_j L, \quad \tilde{c}' = c' L, \quad \tilde{\lambda} = \lambda L. \tag{B1}$$

Eqs.(7,8) then become

$$\frac{\tilde{k}_j - \tilde{\lambda} + i\tilde{c}'}{k_j - \lambda - i\tilde{c}'} = \exp(i\tilde{k}_j), \tag{B2}$$

$$\prod_{j=1}^N \frac{\tilde{k}_j - \tilde{\lambda} + i\tilde{c}'}{k_j - \lambda - i\tilde{c}'} = 1, \tag{B3}$$

Without causing confusion and for convenience, we drop tilde first and recover it at the end. That is that we now use

$$\frac{k_j - \lambda + ic'}{k_j - \lambda - ic'} = \exp(ik_j), \tag{B4}$$

$$\prod_{j=1}^N \frac{k_j - \lambda + ic'}{k_j - \lambda - ic'} = 1. \tag{B5}$$

There are infinite solutions. We focus on the solutions near the ground state.

### 1. Weak interaction limit

In the ground state of the non-interacting case  $c = 0$ , the up-spin fermions occupy the momentum states  $\{0, \pm 1, \pm 2, \dots, \pm(N-2)/2\}2\pi$  ( $N$  is assumed to be even in the main text) and the sole down-spin fermion has zero momentum. The small excitation state correspond to that the down-spin takes up non-zero momentum. In all these states, there is only one momentum state that is occupied by both up-spin and down-spin fermions. If this momentum state is  $k_p = 2n_p\pi$ , the total momentum  $q$  of the system is given by this momentum and we have  $q = 2n_p\pi$ . Our focus is on these states.

We now turn on a small attractive interaction. The common momentum shared by the up and down-spin is split into two  $k_p^\pm = p \pm i\beta$  while all the other momenta are shifted as  $k_j = 2n_j\pi + \delta k_j$ . Our aim is to compute  $p$ ,  $\beta$ , and  $\delta k_j$ . Note that despite of the change of each momentum  $k_j$  by the interaction, the total momentum  $q$  of the system remains unchanged. We still have  $q = 2n_p\pi$ . This is because that the interaction is between fermions and is incapable of changing the total momentum.

For  $k_j = 2n_j\pi + \delta k_j$ , we have from Eq.(B4)

$$\exp(ip - \beta) = \frac{p - \lambda + i(\beta + c')}{p - \lambda + i(\beta - c')}, \tag{B6}$$

$$\exp(ip + \beta) = \frac{p - \lambda - i(\beta - c')}{p - \lambda - i(\beta + c')}, \tag{B7}$$

which lead to

$$\tan p = \frac{2c'(p - \lambda)}{(p - \lambda)^2 + (\lambda^2 - c'^2)}, \tag{B8}$$

$$(p - \lambda)^2 = -\beta^2 - c'^2 + c' \frac{2\lambda(e^{-2\beta} + 1)}{e^{-2\beta} - 1}. \tag{B9}$$

So, when  $c \rightarrow 0$ ,  $(p - \lambda) \rightarrow 0$ . Since  $p = 2n_p\pi$  at  $c = 0$ , we know that  $\lambda \rightarrow 2n_p\pi$  as  $c \rightarrow 0$ . This means that

$k_j - \lambda \sim 2\pi$ . Knowing this fact of the weak coupling limit, we have from Eq.(B4) to the first order of  $c$

$$\frac{1 + \frac{ic'}{k_j - \lambda}}{1 - \frac{ic'}{k_j - \lambda}} = \exp(ik_j), \quad (\text{B10})$$

$$1 + \frac{ic}{2(n_j - n_p)\pi} \approx 1 + i(k_j - 2n_j\pi), \quad (\text{B11})$$

We then have

$$k_j \approx 2n_j\pi - \frac{|c|}{2(n_j - n_p)\pi}. \quad (\text{B12})$$

As the total momentum  $q = 2p + \sum_j k_j = 2n_p\pi$ , we have

$$p \approx 2n_p\pi + \frac{1}{2} \sum_{j=1}^{N-2} \frac{|c|}{2(n_j - n_p)\pi}. \quad (\text{B13})$$

Note that in the above summation and any following summation involving  $n_j - n_p$  we always assume that  $n_j \neq n_p$ .

After cancelling  $\lambda$  from Eqs.(B8,B9) we have

$$\begin{aligned} & -\beta^2 - c'^2 + c' \frac{2\beta}{e^{-2\beta} - 1} (e^{-2\beta} + 1) \\ & = \tan^2 p \left( \frac{e^{-2\beta} + 1}{e^{-2\beta} - 1} \beta - c' \right)^2. \end{aligned} \quad (\text{B14})$$

Since  $\tan^2 p = \tan^2(p - 2n_p\pi) \sim c^2$ , we have to have  $\beta \approx \sqrt{|c|}$ . So, the system energy up to the first order of  $c$  is

$$\begin{aligned} E &= \frac{\hbar^2}{2m} \left( -2\beta^2 + 2p^2 + \sum_{j=1}^{N-2} k_j^2 \right) \\ &\approx -\frac{\hbar^2}{2m} \frac{2(N-1)|c|}{L} + \frac{\hbar^2 q^2}{2m} + E_0, \end{aligned} \quad (\text{B15})$$

We have now computed  $p$ ,  $k_j$  and  $\beta$  to the lowest order. We next try to compute  $p$ ,  $k_j$  and  $\beta$  to the next order. We write

$$p = 2n_p\pi + p^{(1)} + p^{(2)} + \dots \quad (\text{B16})$$

$$k_j = 2n_j\pi + k_j^{(1)} + k_j^{(2)} + \dots \quad (\text{B17})$$

$$\beta = \sqrt{|c|} + \beta^{(2)}, \quad (\text{B18})$$

where  $p^{(1)}$  and  $k_j^{(1)}$  are already computed in the above. We have from Eq.(B10)

$$\begin{aligned} & \frac{1 + \frac{ic'}{2n_j\pi + k_j^{(1)} - 2n_p\pi - 2p^{(1)}}}{1 - \frac{ic'}{2n_j\pi + k_j^{(1)} - 2n_p\pi - 2p^{(1)}}} \approx \exp(ik_j) \quad (\text{B19}) \\ & \frac{2ic'}{2n_j\pi - 2n_p\pi} - \frac{2i(k_j^{(1)} - 2p^{(1)})c'}{(2n_j\pi - 2n_p\pi)^2} \\ & + 2 \left( \frac{ic'}{2n_j\pi - 2n_p\pi} \right)^2 \approx i(k_j^{(1)} + k_j^{(2)}) - \frac{(k_j^{(1)})^2}{2}. \end{aligned} \quad (\text{B20})$$

This leads to

$$\begin{aligned} k_j^{(2)} &= -\frac{c^2}{8(n_j - n_p)^2\pi^3} \left\{ \frac{1}{n_j - n_p} \right. \\ & \left. + \sum_{i=1}^{N-2} \frac{1}{n_i - n_p} \right\}. \end{aligned} \quad (\text{B21})$$

We again use that  $q = 2p + \sum_j k_j = 2n_p\pi$  to find

$$\begin{aligned} p^{(2)} &= \frac{c^2}{16\pi^3} \left\{ \sum_{j=1}^{N-2} \frac{1}{(n_j - n_p)^3} \right. \\ & \left. + \sum_{j=1}^{N-2} \sum_{i=1}^{N-2} \frac{1}{(n_j - n_p)^2(n_i - n_p)} \right\}. \end{aligned} \quad (\text{B22})$$

Through the Taylor expansion, we have from Eq.(B14)

$$-\beta^2 - c'^2 - 2c' \frac{1 - \beta + \beta^2}{1 - \beta + 2\beta^2/3} \approx (p^{(1)})^2, \quad (\text{B23})$$

$$-\beta^2 - c'^2 + |c|(1 + \frac{\beta^2}{3}) \approx (p^{(1)})^2. \quad (\text{B24})$$

From this we obtain

$$\beta^{(2)} \approx \frac{|c|^{3/2}}{24} - \frac{(p^{(1)})^2}{2\sqrt{|c|}}. \quad (\text{B25})$$

With the above results, we have the second-order energy

$$E^{(2)} = -\frac{\hbar^2}{2m} \left\{ \frac{c^2}{6} + \frac{c^2}{2\pi^2} \sum_{j=1}^{N-2} \frac{1}{(n_j - n_p)^2} \right\}. \quad (\text{B26})$$

Note that in the above summation we have  $n_j \neq n_p$  and the units have been restored. It is not clear how to extract a term which is proportional to  $n_p^2$  and obtain the second order correction to the effective mass.

## 2. Strong interaction limit

We now consider the strong coupling limit, i.e.,  $|c| \gg 1$ , where we compute everything up to the first order of  $1/|c|$ . In this limit we have  $\beta \gg 1$  and thus  $e^{-2\beta} \ll 1$ . From Eq.(B9), we have

$$\begin{aligned} (p - \lambda)^2 &\approx -\beta^2 - c'^2 - 2\beta c'(1 + e^{-2\beta})^2 \\ &\approx -(\beta + c')^2 - 4\beta c' e^{-2\beta} \\ &\approx -(\beta + c')^2. \end{aligned} \quad (\text{B27})$$

This gives us

$$p \approx \lambda, \quad \beta \approx -c' = |c|/2. \quad (\text{B28})$$

In the limit of  $|c| \rightarrow \infty$ , if the system is stable near the ground state,  $k_j$ 's and  $p$  must be finite. With Eq.(B4) this implies that  $\exp(ik_j) \rightarrow -1$  and  $k_j \rightarrow n_j\pi$  with  $n_j$  being an odd integer. Combining Eq.(B4) and Eq.(B5)

we have  $e^{-2ip} = e^{i\sum_j k_j}$ . This means that we have  $e^{2ip} \rightarrow (-1)^{N-2}$  in the limit of  $|c| \rightarrow \infty$ . As  $N$  is even (which is assumed in this work), we have  $p \rightarrow n_p\pi$  with  $n_p$  being an arbitrary integer.

With the above results we have

$$\exp(ik_j) \approx \frac{k_j - p + ic'}{k_j - p - ic'} \quad (\text{B29})$$

$$1 + i[k_j - n_j\pi] \approx \frac{-i(n_j - n_p)\pi/c' + 1}{i(n_j - n_p)\pi/c' + 1} \quad (\text{B30})$$

$$k_j \approx n_j\pi + \frac{4\pi(n_j - n_p)}{|c|}. \quad (\text{B31})$$

with  $n_j$  being odd integers. As  $q = \sum_j k_j + 2p = 2n_p\pi$ , we have

$$p \approx n_p\pi - \sum_{j=1}^{N-2} \frac{2n_j\pi}{|c|} + \frac{2(N-2)n_p\pi}{|c|}. \quad (\text{B32})$$

From all the above results, it is clear that the ground

state of the system in the limit of  $|c| \rightarrow \infty$  corresponds to that  $n_j$ 's take values of  $\pm 1, \pm 3, \pm 5, \dots, \pm(N-3)$  while  $n_p = 0$ .  $n_p \neq 0$  corresponds to excited states.

So the system's energy up to the order  $1/|c|$  is

$$\begin{aligned} E &= \frac{\hbar^2}{2m} \left( -2\beta^2 + 2p^2 + \sum_{j=1}^{N-2} k_j^2 \right) \\ &= -\frac{\hbar^2}{2m} \left[ \frac{c^2}{2} + \left( 1 + \frac{8}{|cL|} \right) \frac{(2N-1)(N-2)\pi^2}{L^2} \right] \\ &\quad + \left[ \frac{1}{2} + \frac{2(N-2)}{|cL|} \right] \frac{\hbar^2 q^2}{2m} + \left( 1 + \frac{8}{|cL|} \right) E_0. \end{aligned} \quad (\text{B33})$$

The effective mass can be extracted from the kinetic part of the energy and it is

$$m^* \approx 2m \left[ 1 - \frac{4(N-2)}{L|c|} \right]. \quad (\text{B34})$$